Published in final edited form as:

*Acc Chem Res*. 2019 December 17; 52(12): 3475–3487. doi:10.1021/acs.accounts.9b00490.

# Synthesis, Transformation, and Utilization of Monodispersed Colloidal Spheres

**Jichuan Qiu**[†], **Pedro H. C. Camargo**[‡], **Unyong Jeong**[§], **Younan Xia**[†,&,*]

[†]The Wallace H. Coulter Department of Biomedical Engineering, Georgia Institute of Technology and Emory University, Atlanta, GA 30332, USA [‡]Department of Chemistry, University of Helsinki, Helsinki, 00014, Finland [§]Department of Materials Science and Engineering, Pohang University of Science and Technology, Pohang, 7900-784, South Korea [&]School of Chemistry and Biochemistry, School of Chemical and Biomolecular Engineering, Georgia Institute of Technology, Atlanta, GA 30332, USA

## Conspectus

Colloidal particles with a spherical shape and diameters in the range of 0.01−1 μm have been a subject of extensive research, with applications in areas such as photonics, electronics, catalysis, drug delivery, and medicine. For most of these applications, it is of critical importance to achieve monodispersity for the size while expanding the diversity in terms of structure and composition. The uniformity in size allows one to establish rigorous correlations between this parameter and the physicochemical properties of the colloidal particles while ensuring experimental repeatability and measurement accuracy. On the other hand, the diversity in structure and composition offers additional handles for tailoring the properties. By switching from the conventional plain, solid structure to a core-shell, hollow, porous, or Janus structure, it offers immediate advantages and creates new opportunities, especially in the context of self-assembly, encapsulation, and controlled release. As for composition, monodispersed colloidal spheres were traditionally limited to amorphous materials such as polystyrene and silica. For metals and semiconducting materials, which are more valuable to applications in photonics, electronics, and catalysis, they tend to crystallize and thus grow anisotropically into non-spherical shapes, especially when their sizes pass 0.1 μm. Taken together, it is no wonder why chemical synthesis of monodispersed colloidal spheres has been a constant theme of research in areas such as colloidal science, materials chemistry, materials science, and soft matter.

In this account, we summarize our efforts over the past two decades in developing solution-phase methods for the facile synthesis of colloidal spheres that are uniform in size, together with a broad range of compositions (including metals and semiconductors) and structures (*e.g.*, solid, core-shell, hollow, porous, and Janus, among others). We start with the synthesis of monodispersed colloidal spheres made of semiconductors, metals with low melting points, and precious metals. Through chemical reactions, these colloidal spheres can be transformed into core-shell or hollow structures with new compositions and properties. Next, we discuss the synthesis of colloidal

[*]Corresponding author: younan.xia@bme.gatech.edu.

The authors declare no competing financial interest.

spheres with a Janus structure while taking a pseudo-spherical shape. Specifically, metal-polymer hybrid particles comprised of one metal nanoparticle partially embedded in the surface of a polymer sphere can be produced through precipitation polymerization in the presence of metal seed. With these Janus particles serving as templates, other types of Janus structures such as hollow spheres with a single hole in the surface can be obtained *via* site-selected deposition. Alternatively, such hollow spheres can be fabricated through a physical transformation process that involves swelling of polymer spheres, followed by freeze-drying. All these synthesis and transformation processes are solution-based, offering flexibility and potential for large-scale production. At the end, we highlight some of the applications enabled by these colloidal spheres, including fabrication of photonic devices, encapsulation, and controlled release for nanomedicine.

## Graphical Abstract

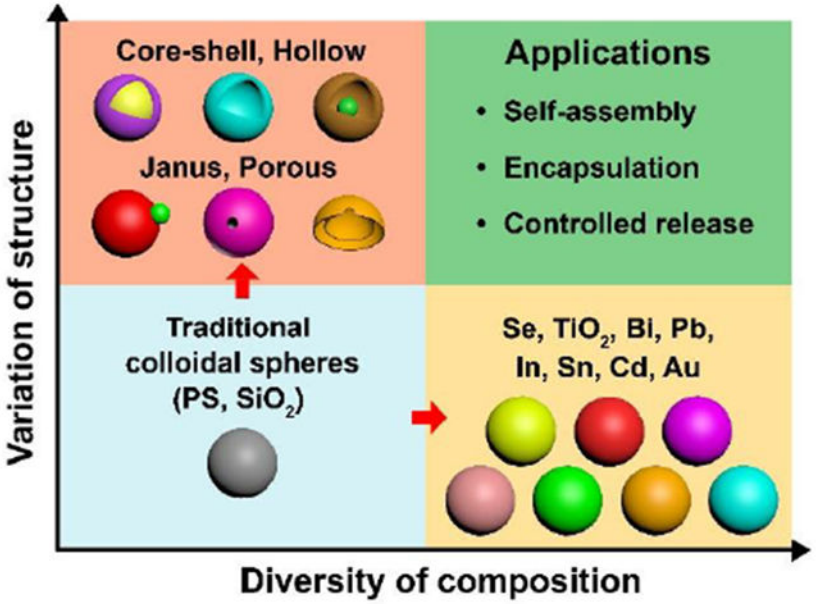


## 1. Introduction

Colloidal particles refer to objects with at least one dimension in the range of 0.01–1 μm, with the upper limit defined by the involvement of Brownian motion. They are typically dispersed in a medium to form a colloidal suspension. The term of “colloid” was coined by Thomas Graham, one of the greatest physical chemists in the 19th century.[1] Although colloidal suspensions have been involved in everyday life since ancient times, for example, in the form of ink or milk, the first documented synthesis only goes back to the work by Michael Faraday in 1856 on Au colloids.[2] The ruby-red color displayed by Faraday’s Au colloids puzzled scientists for many decades and later triggered the development of surface plasmonics, one of the forerunners of nanoscience and nanotechnology. Although a colloidal particle can take many different shapes, the spherical shape has received the most attention owning to its simplicity.[3] In terms of surface energy, colloidal spheres represent a thermodynamically favorable state and are therefore easy to synthesize. The spherical shape

also makes them ideal building blocks for the fabrication of long-range ordered structures through self-assembly or crystallization.

For colloidal spheres, one can easily define them using three parameters: size, composition, and structure. Typically, their physicochemical properties are strongly correlated with particle size and a narrow distribution in size is essential to the precise description of their properties. Traditionally, the availability of monodispersed colloidal spheres has been restricted to polystyrene and silica, two amorphous, dielectric materials with very limited electronic and optical properties.[3,4] There is always a strong demand to increase the diversity of composition by including materials such as semiconductors and metals in order to access their unique electronic, optical, optoelectric, magnetic, and thermoelectric properties.[4] As for structure, it can be utilized to tailor the properties of colloidal spheres by simply moving from the conventional solid structure to core-shell, hollow, porous, and Janus structures. Taken together, it has been a constant theme of research to develop methods for the chemical synthesis of monodispersed colloidal spheres with diverse, and yet well-controlled, compositions and/or structures.

This Account focuses on the efforts from our own group towards the development of solution-phase methods for the facile synthesis of colloidal spheres with uniform sizes while they can be engineered to take a wealth of compositions and structures. We start with materials that can be processed as colloidal spheres with a solid structure and then discuss how to transform them into core-shell or hollow spheres without losing the size uniformity. We also discuss the preparation of colloidal particles displaying an asymmetric Janus structure while taking a pseudo-spherical shape. Finally, we highlight several properties and applications enabled by these new colloidal spheres in the context of crystallization, encapsulation, and controlled release.

## 2. Solid Colloidal Spheres with Diverse Compositions

This section focuses on the synthesis of uniform colloidal solid spheres from four new types of materials, including amorphous selenium (*a*-Se),[5] titania ($TiO_2$),[6] metals with low melting points (*e.g.*, Bi, Pb, In, Sn, Cd, and their alloys),[7,8] and gold (Au).[9] To work with such a broad range of materials, we had to explore different methods, including bottom-up and top-down, as well as successive, seed-mediated growth. When an amorphous material is involved, the spherical shape is naturally obtained because of its lowest total surface area relative to all other shapes. In the case of a crystalline material, one has to eliminate the use of any facet-specific capping agent, while optimizing the growth kinetics, in order to obtain spherical particles.[10–12] For all syntheses, a uniform size can be achieved for the products by temporally separating growth from nucleation.[3]

The preparation of *a*-Se colloidal spheres follows a typical bottom-up approach, in which a precursor compound is reduced or decomposed to generate the atomic building blocks that then nucleate and grow into colloidal spheres. Figure 1A shows an SEM image of *a*-Se colloidal spheres with a diameter of 0.29 μm, which were obtained through the reduction of selenious acid ($HSeO_3$) by hydrazine ($N_2H_4$) at room temperature, with ethylene glycol (EG) serving as a solvent.[5] In this protocol, the reaction was held below the glass transition

temperature ($T_g$) of Se (*ca.* 31 °C) to ensure that Se was precipitated out in the amorphous form. As such, the spherical shape was favored due to the necessity to minimize the surface area. In addition, the use of a viscous solvent like EG, instead of water, allowed for a better control over the transport of Se "monomers", the number of nucleation events, and the growth kinetics, leading to the production of monodispersed samples. For this system, the diameter of the *a*-Se colloidal spheres could be readily controlled in the range of 0.09–0.42 μm by simply varying the molar ratio of $H_2SeO_3$ to $N_2H_4$.[5]

For $TiO_2$, its colloidal spheres can also be prepared using a bottom-up approach involving the hydrolysis of a precursor compound. However, the formation of uniform samples was troubled by the fast hydrolysis kinetics of the conventional precursors based on metal alkoxides.[13] At a fast hydrolysis rate, it is difficult to temporally separate growth from nucleation for the formation of colloidal spheres in one size population only. To address this issue, we switched to a precursor compound based on titanium glycolate, which was much more resistant to hydrolysis relative to titanium alkoxides.[6] The monodispersed colloidal spheres of titanium glycolate were obtained through a homogeneous nucleation and growth process by pouring the glycolate-based precursor into an acetone bath containing a small (*ca.* 0.3 %) amount of water. Figure 1B shows an SEM of the as-obtained 0.32 μm-titanium glycolate spheres. Their diameters could be tuned in the range of 0.2−0.5 μm by changing the precursor concentration. The titanium glycolate could then be converted to $TiO_2$ without altering the spherical shape through calcination in air at 500 °C (for anatase) or 900 °C (for rutile), see the insets in Figure 1B.

Metals with relatively low melting point, including Bi, Pb, In, Sn, Cd, and their alloys, can be prepared as monodispersed colloidal spheres using both bottom-up and top-down approaches. The bottom-up approach involves the decomposition of a precursor in a solvent at a temperature above the melting point of the metal.[7,8] As a result, the generated metal was retained in the liquid state during the entire growth process and finally formed into uniform spherical droplets. The droplets were then converted into solid spheres upon quenching through pouring the reaction mixture into a cold solvent bath. Figure 1C shows an SEM image of the 0.19-μm Pb colloidal spheres obtained by decomposing lead acetate in tetra(ethylene glycol) (TEG) at 320 °C, under $N_2$ protection, and in the presence of PVP as a stabilizer.[7] The diameter of the Pb spheres could be controlled in the range of 0.1–0.6 μm by adjusting the concentration of lead acetate. As for the top-down approach, powders of the metal of interest were directly melted in a solvent and emulsified under rapid magnetic stirring to generate uniform droplets of the melted metal.[7] Figure 1D shows an SEM image of the 0.305-μm Bi colloidal spheres produced by adding Bi powders into boiling di(ethylene glycol) (DEG) in the presence of PVP, followed by quenching with cold ethanol. Using a similar approach, uniform colloidal spheres made of Cd-Pd alloys (Figure 1E) have also been obtained by adding both Cd and Pd powders into boiling DEG.[7]

To obtain colloidal spheres made of a precious metal such as Au, we developed a successive, seed-mediated growth method to achieve both spherical shapes and narrow size distributions.[9,14] This method allows for the separation of growth from nucleation, as well as the precise control over the growth kinetics. In a typical synthesis, 10-nm Au nanospheres were firstly prepared by taking Au clusters as the initial seeds. The as-obtained 10-nm Au

nanospheres then served as seeds for the growth of 46-nm Au nanospheres. Finally, Au colloidal spheres over 0.1 μm could be generated through another round of seed-mediated growth involving the 46-nm Au nanospheres as seeds. Figure 1F shows a TEM image of the as-obtained 0.15-μm Au colloidal spheres. In this process, both the involvement of slow growth kinetics and the absence of halide ions capable of selectively capping a specific type of facet were critical to the formation of spherical particles.[9] The growth kinetics could be slowed down by injecting the Au precursor solution dropwise and/or reducing the concentration of the reductant.

## 3. Colloidal Spheres with a Core-Shell or Hollow Structure

Another promising strategy for increasing the diversity, complexity, and functionality of colloidal spheres involves the transformation of existing samples into new materials (*via* a change in composition) and structures (*via* a change in morphology). Here we focus on how to transform some of the solid colloidal spheres in Section 2 into core-shell and hollow morphologies through chemical reactions. Starting from uniform *a*-Se spheres, for example, a combination of a template-engaged reaction and cation-exchange could be used to produce core-shell spheres displaying a wealth of compositions (Figure 2A).[15–17] In this transformation, $Ag^+$ ions were reduced to $Ag^0$ by EG at room temperature, which reacted with *a*-Se *in situ* to generate a $Ag_2Se$ shell over the surface of each colloidal sphere for the production of an *a*-Se@$Ag_2Se$ core-shell sphere (Figure 2B). The $Ag_2Se$ shell could then be converted into a variety of MSe (M = Zn, Cd, and Pb) chalcogenides *via* cation-exchange between $Ag^+$ and $Zn^{2+}$, $Cd^{2+}$, and $Pb^{2+}$ ions, respectively.[16,17] Figure 2, C−E, shows SEM and TEM (insets) images of the *a*-Se@MSe core-shell spheres, confirming the ability to preserve both the spherical shape and size uniformity during the reaction and cation-exchange process.

We also explored Pb colloidal spheres as a template for the synthesis of semiconductor hollow spheres (Figure 3A).[18] We reacted Pb colloidal spheres with sulfur at 300 °C in Ar for the production of Pb@PbS core-shell spheres. Interestingly, as the reaction progressed, a void would be formed and then enlarged inside each particle as a result of the Kirkendall effect.[19] The Kirkendall effect occurs when the mutual diffusion flux ($J$) from the core to the shell ($J_{core}$) is greater than the flux in the opposite direction ($J_{shell}$).[19] In this case, the interface between the core and the shell materials moves outward from the core and leaves a vacancy behind, which is accumulated in the core for the generation of a gradually enlarged void until the reaction is terminated. Figures 3, B and C, shows SEM and TEM images, respectively, of the PbS hollow spheres obtained after the Pb had been completely reacted with S, confirming the preservation of both spherical shape and uniform size.[18]

Using a different approach, we developed a method for the facile preparation of hollow spheres containing a movable core in the interior (Figure 3D).[20] Typically, a conformal silica shell was deposited on each Au nanoparticle *via* the Stöber method, followed by the attachment of a sub-monolayer of [(chloromethyl)phenylethyl]-trichlorosilane (CMTS) on the silica surface *via* the siloxane linkage. The CMTS could initiate the atom transfer radical polymerization (ATRP) of benzyl methacrylate, resulting in the formation of a shell of poly(benzyl methacrylate) (PBzMA) on the surface of each particle. After removal of the

silica with aqueous hydrofluoric acid, PBzMA hollow spheres containing movable Au cores were obtained (Figure 3E). Based on the TEM image in Figure 3F, the thickness of the PBzMA shell was *ca.* 22 nm and it could be adjusted by controlling the polymerization conditions.

## 4. Colloidal Spheres with a Janus Structure

Janus colloidal particles with an asymmetric structure have received ever increasing attention over the past two decades.[21] This new class of colloidal materials is attractive for applications related to dynamic assembly, stabilization of oil-in-water or water-in-oil emulsions, catalysis, and fabrication of active motors and multifunctional optical, electronic, and sensing devices.[21–24] Although much effort has been directed towards the synthesis of Janus colloidal particles, most of the methods involve complicated procedures. To address this problem, we have developed a method for facile, scalable production of a unique type of Janus particles characterized by a metal-polymer hybrid composition and a pseudo-spherical shape.[25–28]

The synthesis of such Janus particles was achieved by introducing metal nanoparticles as seeds for the precipitation polymerization of polystyrene (PS). Figure 4A shows a schematic of the protocol for the production of Au-PS Janus particles.[25] In a typical process, PS polymerization was initiated by potassium persulphate (KPS) in a mixture of ethanol and water containing styrene, divinylbenzene (DVB), and 4-styrenesulfonic acid sodium salt. After the polymerization had started for 2 min, Au nanoparticles were introduced serving as seeds. PS would then nucleate and grow from one side of each Au nanoparticle, eventually leading to the formation of Au-PS spheres with a Janus structure. TEM images of the reaction intermediates in Figure 4B–D validate the growth process of PS on Au nanoparticles. Figure 4E shows the final Au-PS Janus products, featuring only one Au nanoparticle partially embedded in the surface of a PS bead. This method could be extended to generate a series of M-PS (M = Au, Pd, and Pt) Janus particles.[26] It is worth noting that initial pattern of polymerization on the metal nanoparticle critically depended on the capping agent, as well as the concentration of DVB, a cross-linker.[26–28] Additionally, the sizes of the PS and metal in a Janus particle could be readily tuned by controlling the polymerization time and employing metal nanoparticles with different sizes, respectively.[26,27]

## 5. Colloidal Hollow Spheres with a Hole on the Surface

We then explored these metal-polymer Janus particles as a template to prepare hollow spheres with a circular opening on the surface. Figure 5A shows the major steps involved in this preparation.[27] A hydrophobic silica precursor, vinyltrimethoxysilane (VTMS), was used to deposit a shell of vinyl-silica on the hydrophobic PS surface only, while exempting the hydrophilic surface terminated in Au. The Au nanoparticle was then etched away using an aqueous solution containing KI and $I_2$,[29] while the PS was removed by calcination at 500 °C or dissolution with an organic solvent such as tetrahydrofuran, with a result of the formation of hollow silica/vinyl silica spheres with a circular opening. Figure 5B shows TEM image of the Au–PS Janus particles containing a 50-nm Au nanoparticle, while Figure 5C shows the SEM and TEM (inset) images of the resultant hollow silica spheres. The hollow silica

spheres had a mean diameter of 0.192 μm, a shell thickness of 16 nm, and a surface hole of 24 nm in size. The diameter of the dedicated hole could be easily tuned by changing the size of Au nanoparticles used for the preparation of Au-PS Janus particles. For example, when 100-nm Au nanoparticles were used to prepare the Au-PS Janus particles (Figure 5D), the surface hole on the final hollow spheres was increased to 62 nm (Figure 5E).[27]

In addition to the templating method, physical transformation of polymer beads can also be used as an alternative method for the fabrication of hollow spheres with an opening.[30–32] In a typical process (Figure 6A),[30] the commercial PS beads were swollen by introducing a good solvent for PS (*e.g.*, toluene or styrene) into their aqueous suspension, followed by freezing with liquid nitrogen. The volumetric shrinkage associated with the cooling process would lead to the migration of both solvent molecules and polymer chains from the interior of the swollen bead towards the surface, leaving behind a small void in the center. By storing the sample in a freezer at a temperature above the melting point of the solvent but below that of water, the solvent could be removed completely while the entire system remaining in the solid state. The flux of solvent evaporation resulted in the formation of a hole in the wall, and the opening could be gradually enlarged due to the migration of polymer chains. Figure 6B shows 0.55-μm PS hollow spheres with an opening of *ca.* 50 nm in diameter produced by swelling 0.48-μm PS beads with 1% aqueous toluene (*v*/*v*) and then freeze-drying.[31] The size of the opening could be easily tuned by varying the degree of swelling, which was mainly determined by the amount of the solvent added into the aqueous suspension. For example, when PS beads were swollen with 5% aqueous toluene (*v*/*v*), the opening was increased to 350 nm (Figure 6C). Meanwhile, the diameter of the PS hollow spheres was increased to 0.65 μm as a result of enhancement in swelling. This protocol has been successfully applied to a variety of amorphous or semi-crystalline polymers, including biocompatible and biodegradable poly(caprolactone) (PCL) and poly(L-lactide) (PLLA).[32] Significantly, the hole on the surface of the polymer hollow spheres could be readily closed through a thermal or solvent-induced annealing process, for the encapsulation of various types of chemicals and materials (see Section 7).

## 6. Hollow Spheres Made of Conducting Polymers

Colloidal hollow spheres made of conducting polymers have great potential in applications related to electrocatalysis, chemical sensing, microelectronics, and optoelectronics.[33,34] However, when they were prepared by coating the conducting polymer over colloidal templates, the products often exhibited a rough surface, with almost no control over the morphology, uniformity, and wall thickness.[34,35] To address these issues, we developed a method for fabricating hollow spheres made of conducting polymers such as polypyrrole (PPy) and polyaniline (PAni) with drastically improvements in uniformity and surface morphology (Figure 7A).[34] The key to the success of this method is to render the surface of PS templates with sulfonic acid groups by treating with concentrated sulfuric acid for the electrostatic adsorption of protonated pyrrole or aniline monomers. A uniform shell of the conducting polymer could then be deposited on the PS surface after the initiation of polymerization. Figure 7B shows an SEM image of PS@PPy core-shell spheres produced from 2 μm-PS beads, demonstrating the uniform size, smooth surface, and spherical shape for the products. After the removal of PS with tetrahydrofuran, colloidal hollow spheres

made of PPy were obtained (see the inset in Figure 7B). We also demonstrated the fabrication of triple-shelled hollow spheres by switching the template from PS solid beads to PS hollow spheres with a hole on the surface (Figure 7C).[35] After removing the PS shell, we obtained PPy hollow spheres characterized by a double-walled shell and an opening on the surface (see inset in Figure 7C).

## 7. Applications of the Colloidal Spheres

The uniform colloidal spheres with a broad range of compositions and structures have opened up new opportunities in terms of application. Colloidal spheres made of metals and semiconductors, for example, can serve as building blocks for the fabrication of metallodielectric or semiconductor photonic crystals. Compared to the traditional photonic crystals made of silica or PS beads, these photonic crystals offer distinctive electrical, optical, magnetic, or thermoelectric properties.[4,36,37] As for colloidal spheres with a Janus structure, they have been explored as building blocks for the fabrication of dimers, trimers, and superlattices. [21,38] The Janus particles could also serve as a stabilizer for the creation of a stable emulsion or as a chemical locomotion system.[23,39,40] For colloidal hollow spheres with an opening on the surface, they have shown outperformance in applications related to encapsulation and controlled release.[41,42] In this section, we only focus on three demonstrations in the context of photonics, encapsulation, and controlled release.

In the first demonstration, we prepared a smart photonic crystal made of Se@$Ag_2Se$ core-shell spheres by taking advantage of the reversible, polymorphic transition of $Ag_2Se$.[15] Below 133 °C, $Ag_2Se$ crystallizes in an orthorhombic structure and acts as a semiconductor. When heated to 133 °C, $Ag_2Se$ transforms into a body-centered cubic structure and becomes a good superionic conductor due to the enhanced mobility of $Ag^+$ and the low activation energy to its diffusion and conduction. To this end, its properties could be tuned by adjusting the structure of $Ag_2Se$. Figure 8A shows a cross-sectional SEM image of the photonic crystal assembled from uniform Se@$Ag_2Se$ core-shell spheres. Figure 8B shows the same sample after it had been heated at 150 °C for 10 min, confirming the preservation of the crystalline lattice. Figure 8C shows the near-infrared (NIR) reflectance spectra recorded from the same sample hold at different temperatures. When the temperature was increased from room temperature to 110, and finally to 150 °C, the peak position would be red-shifted from 1392 to 1415, and finally to 1497 nm, as the $Ag_2Se$ shells underwent a phase transition from orthorhombic to the body-centered cubic structure. Interestingly, the peak would shift back to 1415 nm when the sample was re-annealed at 110 °C. Taken together, one could reversibly tune the optical properties of the phonic crystals by changing the annealing temperature.

In the second demonstration, colloidal hollow spheres with an opening on the surface were used to encapsulate imaging contrast agents. The opening allowed us to easily and quickly load a wide variety of functional components, including molecular species, biomacromolecules, and even nanoparticles, into the interior of the hollow particles. [27,30–32,41] Figure 9A schematically shows the encapsulation of different types of imaging contrast agents into PS hollow spheres.[41] The hole on the surface made it very easy and straightforward to load essentially all sorts of contrast agents. Afterwards, the hole could be

sealed by annealing the system at a temperature slightly above the $T_g$ of PS. Figure 9, B−D, shows TEM images of PS hollow spheres after the encapsulation of ioversol at different concentrations. The encapsulated ioversol could serve as an iodinated contrast compound (ICC) for X-ray computed tomography imaging. We have also demonstrated the feasibility to use this method for the encapsulation of other types of contrast agents, including perfluorooctane (PFO) for magnetic resonance imaging (MRI) and NaCl microcrystals for thermoacoustic tomography (TAT) imaging.[41]

The opening on the surface of hollow spheres could also be employed as a smart gate for the controlled release of drugs. We demonstrated this concept by encapsulating a phase-changing material (PCM), together with an anticancer drug and a NIR dye, into the hollow silica spheres with an opening on the surface for NIR-triggered release (Figure 10A).[27] A mixture containing two natural fatty acids (the PCM), doxorubicin (DOX), and indocyanine green (ICG) in dimethyl sulfoxide was firstly loaded into the hollow silica. After discarding the unloaded materials by centrifugation, the PCM was solidified by introducing water due to the immiscibility between them. The solid PCM could keep both DOX and ICG in the hollow spheres. Upon ICG-enabled photothermal heating, the PCM would be melted to undergo a phase transition from solid to liquid, triggering the release of payloads through the hole.[43–45] The loaded anticancer drug could be controllably released inside tumor cells by NIR laser irradiation. As shown in Figure 10B, the DOX loaded in the hollow spheres were concentrated outside the nuclei before laser irradiation. Upon exposure to an 808-nm laser, the DOX was released from the silica hollow spheres, as indicated by the emergence of red fluorescence in the nuclei (Figure 10C). Furthermore, the cumulative release amount of DOX could be manipulated by varying the duration of laser irradiation (Figure 10D).

## 8. Concluding Remarks

To expand the diversity of colloidal spheres, we have developed a number of solution-based methods for the synthesis of uniform samples embracing new compositions and structures. These methods not only allow one to readily produce a wealth of novel colloidal spheres, but also offer flexibility and potential for large-scale production. These new colloidal spheres have shown great performance in a set of applications from assembly to encapsulation and drug delivery. There is no doubt that the research on colloidal spheres will continue to develop strongly, with contributions from chemists, material scientists, physicists, and engineers. Although a number of semiconductors and metals have been prepared as monodispersed colloidal spheres, it is still difficult to work with the vast majority of inorganic materials because of the complications brought up by their crystalline structures. To this end, incorporation of other functional molecules or materials into existing particles offers an effective strategy to further diversify the composition and broaden the function of colloidal spheres. For example, it was reported that superparamagnetic nanoparticles could be incorporated into the *a*-Se spheres during their synthesis to obtain superparamagnetic colloidal spheres more responsive to the external magnetic field.[46–49] On the other hand, tailoring the functional groups on the surface of colloidal spheres offers another opportunity to expand their properties and thus enhance their performance in various applications. Taken together, it is of key importance to have tight controls over the size, composition, structure, and surface functional group of colloidal spheres. It is hoped that readers will enjoy the

colloidal materials and synthetic methods discussed in this Account and perhaps find the inspiration to push the materials a step further toward industrial applications.

## ACKNOWLEDGMENTS

This work was supported in part by research grants from the NSF, NIH, and ONR. It was also supported by start-up funds from the University of Washington, Washington University in St. Louis, and the Georgia Institute of Technology. We are grateful to our coworkers and collaborators for their invaluable contributions to this project.

## Biographical Information

**Jichuan Qiu** received his Ph.D. in materials chemistry and physics from Shandong University in 2018 with Prof. Hong Liu. He joined the Xia group as a visiting graduate student in October 2016 and then continued as a postdoctoral fellow since December 2018.

**Pedro H. C. Camargo** received his Ph.D. in biomedical engineering from Washington University in St. Louis in 2009 with Prof. Younan Xia. He is currently a full professor of chemistry at the University of Helsinki.

**Unyong Jeong** received his Ph.D. in polymer physics from Pohang University of Science and Technology (POSTECH) in 2003. He then worked as a postdoctoral fellow in the Xia group at the University of Washington (Seattle) from 2003 to 2005. He is currently a full professor of materials science and engineering at POSTECH.

**Younan Xia** received his B.S. from the University of Science and Technology of China in 1987. He received his M.S. in 1993 from the University of Pennsylvania (with Prof. Alan G. MacDiarmid) and his Ph.D. in 1996 from Harvard University (with Prof. George M. Whitesides). He started as an assistant professor of chemistry in 1997 at the University of Washington (Seattle) and was promoted to associate professor and professor in 2002 and 2004, respectively. He joined Washington University in St. Louis in 2007 as the James M. McKelvey Professor of Advanced Materials in the Department of Biomedical Engineering. Since January 2012 he has been the holder of the Brock Family Chair and the GRA Eminent Scholar in Nanomedicine at Georgia Tech, with joint appointments in the Department of Biomedical Engineering, School of Chemistry & Biochemistry, and School of Chemical & Biomolecular Engineering. His research interests include nanomaterials, catalysis, biomaterials, nanomedicine, regenerative medicine, and colloidal science.

## REFERENCES

(1). Graham Th. Liquid Diffusion Applied to Analysis. Phil. Trans. Roy. Soc. Lond 1861, 151, 183–224.

(2). Faraday M The Bakerian Lecture: Experimental Relations of Gold (and Other Metals) to Light. Phil. Trans. Roy. Soc. Lond 1857, 147, 145–181.

(3). Xia Y; Gates B; Yin Y; Lu Y Monodispersed Colloidal Spheres: Old Materials with New Applications. Adv. Mater 2000, 12, 693–713.

(4). Jeong U; Wang Y; Ibisate M; Xia Y Some New Developments in the Synthesis, Functionalization, and Utilization of Monodisperse Colloidal Spheres. Adv. Funct. Mater 2005, 15, 1907–1921.

(5). Jeong U; Xia Y Synthesis and Crystallization of Monodisperse Spherical Colloids of Amorphous Selenium. Adv. Mater 2005, 17, 102–106.

(6). Jiang X; Herricks T; Xia Y Monodispersed Spherical Colloids of Titania: Synthesis, Characterization, and Crystallization. Adv. Mater 2003, 15, 1205–1209.

(7). Wang Y; Xia Y Bottom-Up and Top-Down Approaches to the Synthesis of Monodispersed Spherical Colloids of Low Melting-Point Metals. Nano Lett. 2004, 4, 2047–2050.

(8). Wang Y; Ibisate M; Li Z-Y; Xia Y Metallodielectric Photonic Crystals Assembled from Monodisperse Spherical Colloids of Bismuth and Lead. Adv. Mater 2006, 18, 471–476.

(9). Zheng Y; Zhong X; Li Z; Xia Y Successive, Seed-Mediated Growth for the Synthesis of Single-Crystal Gold Nanospheres with Uniform Diameters Controlled in the Range of 5-150 nm. Part. Part. Syst. Charact 2014, 31, 266–273.

(10). Xia Y; Xia X; Peng H-C Shape-Controlled Synthesis of Colloidal Metal Nanocrystals: Thermodynamic Versus Kinetic Products. J. Am. Chem. Soc 2015, 137, 7947–7966. [PubMed: 26020837]

(11). Xia Y; Gilroy KD; Peng H-C; Xia X Seed-Mediated Growth of Colloidal Metal Nanocrystals. Angew. Chem., Int. Ed 2017, 56, 60–95.

(12). Huo D; Kim MJ; Lyu Z; Shi Y; Wiley BJ; Xia Y One-Dimensional Metal Nanostructures: From Colloidal Syntheses to Applications. Chem. Rev 2019, 119, 8972–9073. [PubMed: 30854849]

(13). Matijević E; Budnik M; Meites L Preparation and Mechanism of Formation of Titanium Dioxide Hydrosols of Narrow Size Distribution. J. Colloid Interface Sci 1977, 61, 302–311.

(14). Zheng Y; Ma Y; Zeng J; Zhong X; Jin M; Li Z-Y; Xia Y Seed-Mediated Synthesis of Single-Crystal Gold Nanospheres with Controlled Diameters in the Range 5-30 nm and their Self-Assembly upon Dilution. Chem. Asian J 2013, 8, 792–799. [PubMed: 23362050]

(15). Jeong U; Xia Y Photonic Crystals with Thermally Switchable Stop Bands Fabricated from Se@$Ag_2Se$ Spherical Colloids. Angew. Chem., Int. Ed 2005, 44, 3099–3103.

(16). Jeong U; Kim J-U; Xia Y; Li Z-Y Monodispersed Spherical Colloids of Se@CdSe: Synthesis and Use as Building Blocks in Fabricating Photonic Crystals. Nano Lett. 2005, 5, 937–942. [PubMed: 15884898]

(17). Camargo PHC; Lee YH; Jeong U; Zou Z; Xia Y Cation Exchange: A Simple and Versatile Route to Inorganic Colloidal Spheres with the Same Size but Different Compositions and Properties. Langmuir 2007, 23, 2985–2992. [PubMed: 17261053]

(18). Wang Y; Cai L; Xia Y Monodisperse Spherical Colloids of Pb and Their Use as Chemical Templates to Produce Hollow Particles. Adv. Mater 2005, 17, 473–477.

(19). Yin Y; Rioux RM; Erdonmez CK; Hughes S; Somorjai GA; Alivisatos AP Formation of Hollow Nanocrystals Through the Nanoscale Kirkendall Effect. Science 2004, 304, 711–714. [PubMed: 15118156]

(20). Kamata K; Lu Y; Xia Y Synthesis and Characterization of Monodispersed Core-Shell Spherical Colloids with Movable Cores. J. Am. Chem. Soc 2003, 125, 2384–2385. [PubMed: 12603113]

(21). Walther A; Müller AHE Janus Particles: Synthesis, Self-Assembly, Physical Properties, and Applications. Chem. Rev 2013, 113, 5194–5261. [PubMed: 23557169]

(22). Gilroy KD; Ruditskiy A; Peng H-C; Qin D; Xia Y Bimetallic Nanocrystals: Syntheses, Properties, and Applications. Chem. Rev 2016, 116, 10414–10472. [PubMed: 27367000]

(23). Yang Z; Wei J; Sobolev YI; Grzybowski BA Systems of Mechanized and Reactive Droplets Powered by Multi-Responsive Surfactants. Nature 2018, 553, 313–318. [PubMed: 29320473]

(24). Huang Z; Gong J; Nie Z Symmetry-Breaking Synthesis of Multicomponent Nanoparticles. Acc. Chem. Res 2019, 52, 1125–1133. [PubMed: 30943008]

(25). Ohnuma A; Cho EC; Camargo PHC; Au L; Ohtani B; Xia Y A Facile Synthesis of Asymmetric Hybrid Colloidal Particles. J. Am. Chem. Soc 2009, 131, 1352–1353. [PubMed: 19140763]

(26). Ohnuma A; Cho EC; Jiang M; Ohtani B; Xia Y Metal−Polymer Hybrid Colloidal Particles with an Eccentric Structure. Langmuir 2009, 25, 13880–13887. [PubMed: 19621917]

(27). Qiu J; Huo D; Xue J; Zhu G; Liu H; Xia Y Encapsulation of a Phase-Change Material in Nanocapsules with a Well-Defined Hole in the Wall for the Controlled Release of Drugs. Angew. Chem., Int. Ed 2019, 58, 10606–10611.

(28). Qiu J; Xie M; Lyu Z; Gilroy KD; Liu H; Xia Y General Approach to the Synthesis of Heterodimers of Metal Nanoparticles through Site-Selected Protection and Growth. Nano Lett. 2019, 19, 6703–6708. [PubMed: 31449753]

(29). Cho EC; Au L; Zhang Q; Xia Y The Effects of Size, Shape, and Surface Functional Group of Gold Nanostructures on Their Adsorption and Internalization by Cells. Small 2010, 6, 517–522. [PubMed: 20029850]

(30). Im SH; Jeong U; Xia Y Polymer Hollow Particles with Controllable Holes in Their Surfaces. Nat. Mater 2005, 4, 671–675. [PubMed: 16086022]

(31). Hyun DC; Lu P; Choi S-I; Jeong U; Xia Y Microscale Polymer Bottles Corked with a Phase-Change Material for Temperature-Controlled Release. Angew. Chem., Int. Ed 2013, 52, 10468–10471.

(32). Jeong U; Im SH; Camargo PHC; Kim JH; Xia Y Microscale Fish Bowls: A New Class of Latex Particles with Hollow Interiors and Engineered Porous Structures in Their Surfaces. Langmuir 2007, 23, 10968–10975. [PubMed: 17910489]

(33). Winther-Jensen B; Winther-Jensen O; Forsyth M; MacFarlane DR High Rates of Oxygen Reduction over a Vapor Phase–Polymerized PEDOT Electrode. Science 2008, 321, 671–674. [PubMed: 18669857]

(34). Bai M-Y; Cheng Y-J; Wickline SA; Xia Y Colloidal Hollow Spheres of Conducting Polymers with Smooth Surface and Uniform, Controllable Sizes. Small 2009, 5, 1747–1752. [PubMed: 19384880]

(35). Bai M-Y; Xia, Y. Facile Synthesis of Double-Shelled Polypyrrole Hollow Particles with a Structure Similar to That of a Thermal Bottle. Macromol. Rapid Commun 2010, 31, 1863–1868. [PubMed: 21567604]

(36). Zhao Y; Shang L; Cheng Y; Gu Z Spherical Colloidal Photonic Crystals. Acc. Chem. Res 2014, 47, 3632–3642. [PubMed: 25393430]

(37). García-Lojo D; Núñez-Sánchez S; Gómez-Graña S; Grzelczak M; Pastoriza-Santos I; Pérez-Juste J; Liz-Marzán LM Plasmonic Supercrystals. Acc. Chem. Res 2019, 52, 1855–1864. [PubMed: 31243968]

(38). Zhang J; Grzybowski BA; Granick S Janus Particle Synthesis, Assembly, and Application. Langmuir 2017, 33, 6964–6977. [PubMed: 28678499]

(39). Kim J-W; Lee D; Shum HC; Weitz DA Colloid Surfactants for Emulsion Stabilization. Adv. Mater 2008, 20, 3239–3243.

(40). Wang W; Chiang T-Y; Velegol D; Mallouk TE Understanding the Efficiency of Autonomous Nano- and Microscale Motors. J. Am. Chem. Soc 2013, 135, 10557–10565. [PubMed: 23795959]

(41). Bai M-Y; Moran CH; Zhang L; Liu C; Zhang Y; Wang LV; Xia Y A Facile and General Method for the Encapsulation of Different Types of Imaging Contrast Agents Within Micrometer-Sized Polymer Beads. Adv. Funct. Mater 2012, 22, 764–770. [PubMed: 31866803]

(42). Si Y; Chen M; Wu L Syntheses and Biomedical Applications of Hollow Micro-/Nano-Spheres with Large-Through-Holes. Chem. Soc. Rev 2016, 45, 690–714. [PubMed: 26658638]

(43). Moon GD; Choi S-W; Cai X; Li W; Cho EC; Jeong U; Wang LV; Xia Y A New Theranostic System Based on Gold Nanocages and Phase-Change Materials with Unique Features for Photoacoustic Imaging and Controlled Release. J. Am. Chem. Soc 2011, 133, 4762–4765. [PubMed: 21401092]

(44). Hyun DC; Levinson NS; Jeong U; Xia Y Emerging Applications of Phase-Change Materials (PCMs): Teaching an Old Dog New Tricks. Angew. Chem., Int. Ed 2014, 53, 3780–3795.

(45). Choi S-W; Zhang Y; Xia Y A Temperature-Sensitive Drug Release System Based on Phase-Change Materials. Angew. Chem., Int. Ed 2010, 49, 7904–7908.

(46). Jeong U; Herricks T; Shahar E; Xia Y Amorphous Se: A New Platform for Synthesizing Superparamagnetic Colloids with Controllable Surfaces. J. Am. Chem. Soc 2005, 127, 1098–1099. [PubMed: 15669838]

(47). Wang Y; Herricks T; Ibisate M; Camargo PHC; Xia Y Synthesis and Characterization of Monodisperse Colloidal Spheres of Pb Containing Superparamagnetic $Fe_3O_4$ Nanoparticles. Chem. Phys. Lett 2007, 436, 213–217.

(48). Camargo PHC; Li Z-Y; Xia Y. Colloidal Building Blocks with Potential for Magnetically Configurable Photonic Crystals. Soft Matter 2007, 3, 1215–1222.

(49). Jeong U; Teng X; Wang Y; Yang H; Xia Y Superparamagnetic Colloids: Controlled Synthesis and Niche Applications. Adv. Mater 2007, 19, 33–60.

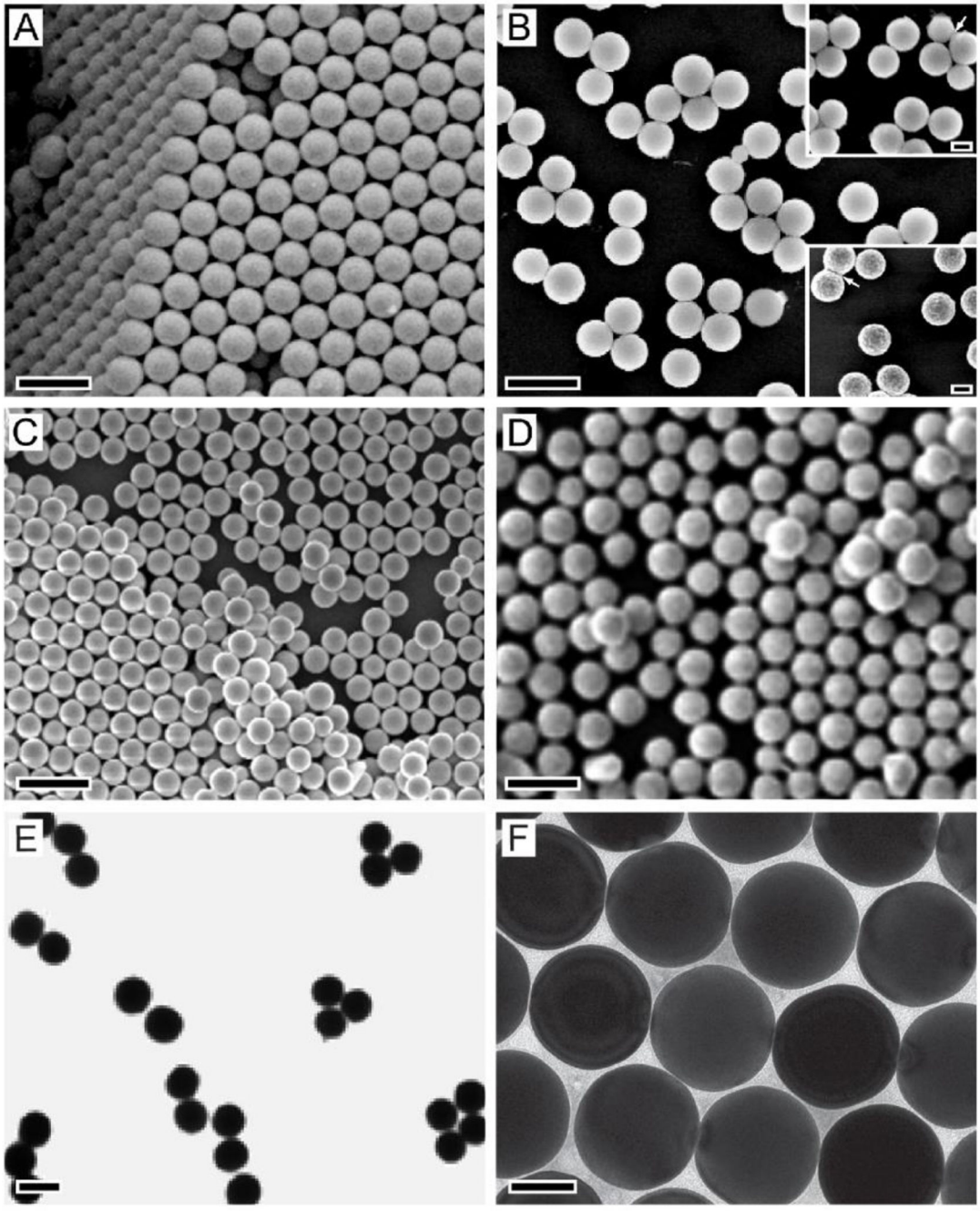


**Figure 1.**

Colloidal spheres with various compositions. (A–D) SEM images of colloidal spheres made of (A) *a*-Se; (B) titanium glycolate, which could be converted to anatase (top inset) and rutile (bottom inset) by calcination at 500 and 950 °C, respectively; (C) Pb; and (D) Bi. (E, F) TEM images of (E) Cd-Pb alloy spheres and (F) Au spheres. Scale bars in (A–E), (F), and the insets of (B) are 0.5, 0.1, and 0.2 μm, respectively. Reproduced with permission from (A) ref 5, (B) ref 6, (C-E) ref 7, and (F) ref 9. Copyright 2005 Wiley-VCH, 2003 Wiley-VCH, 2004 American Chemical Society, and 2014 Wiley-VCH, respectively.

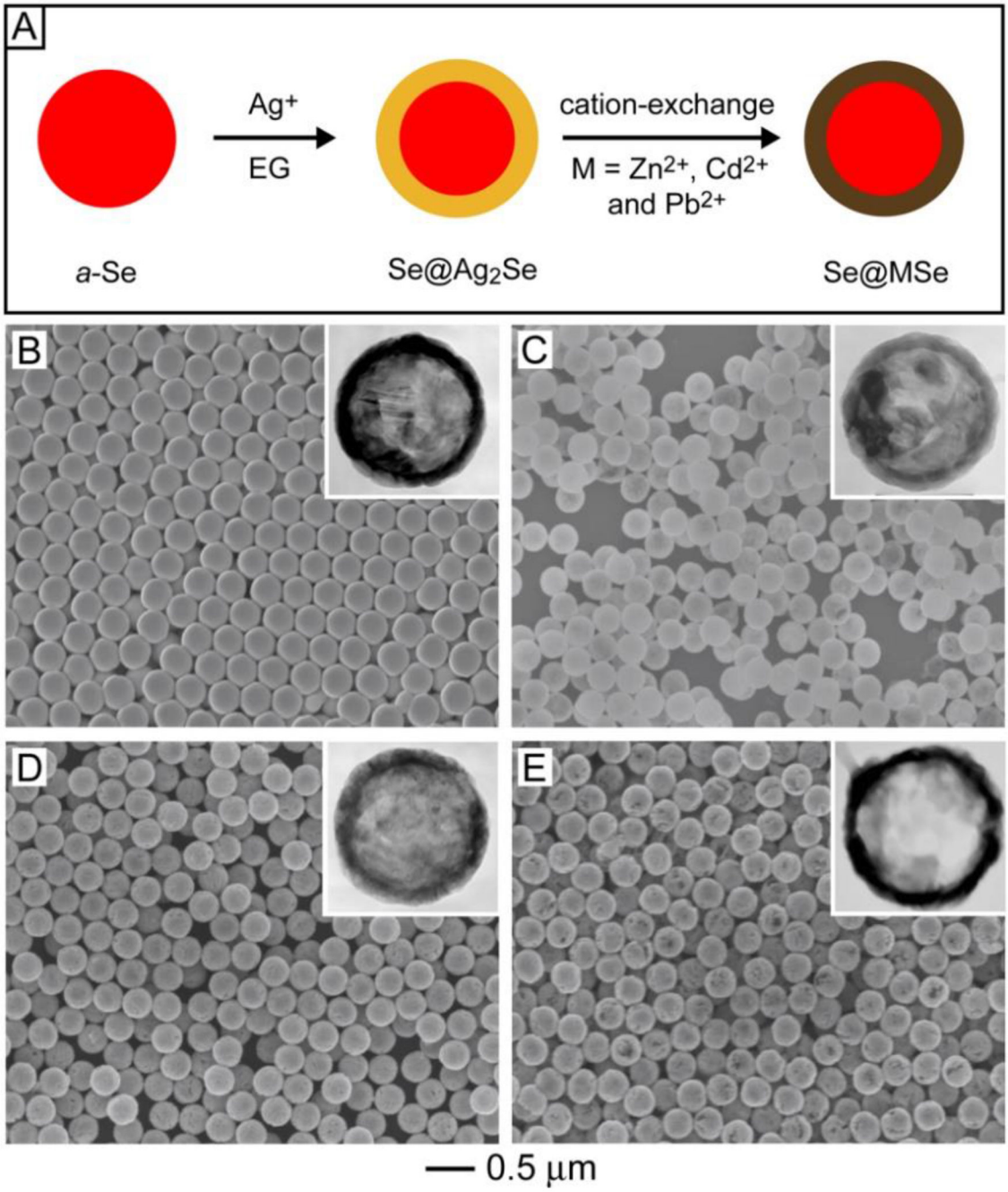


**Figure 2.**

(A) Schematic showing the transformation of *a*-Se colloidal spheres into Se@$Ag_2$Se and Se@MSe (M = Zn, Cd, and Pb) core-shell spheres through a combination of template-engaged reaction and cation exchange. (B–E) SEM images of core-shell spheres made of (B) Se@$Ag_2$Se, (C) Se@ZnSe, (D) Se@CdSe, and (E) Se@PbSe. The insets show TEM images of the corresponding samples after the *a*-Se cores had been removed with hydrazine. Reproduced with permission from ref 17. Copyright 2007 American Chemical Society.

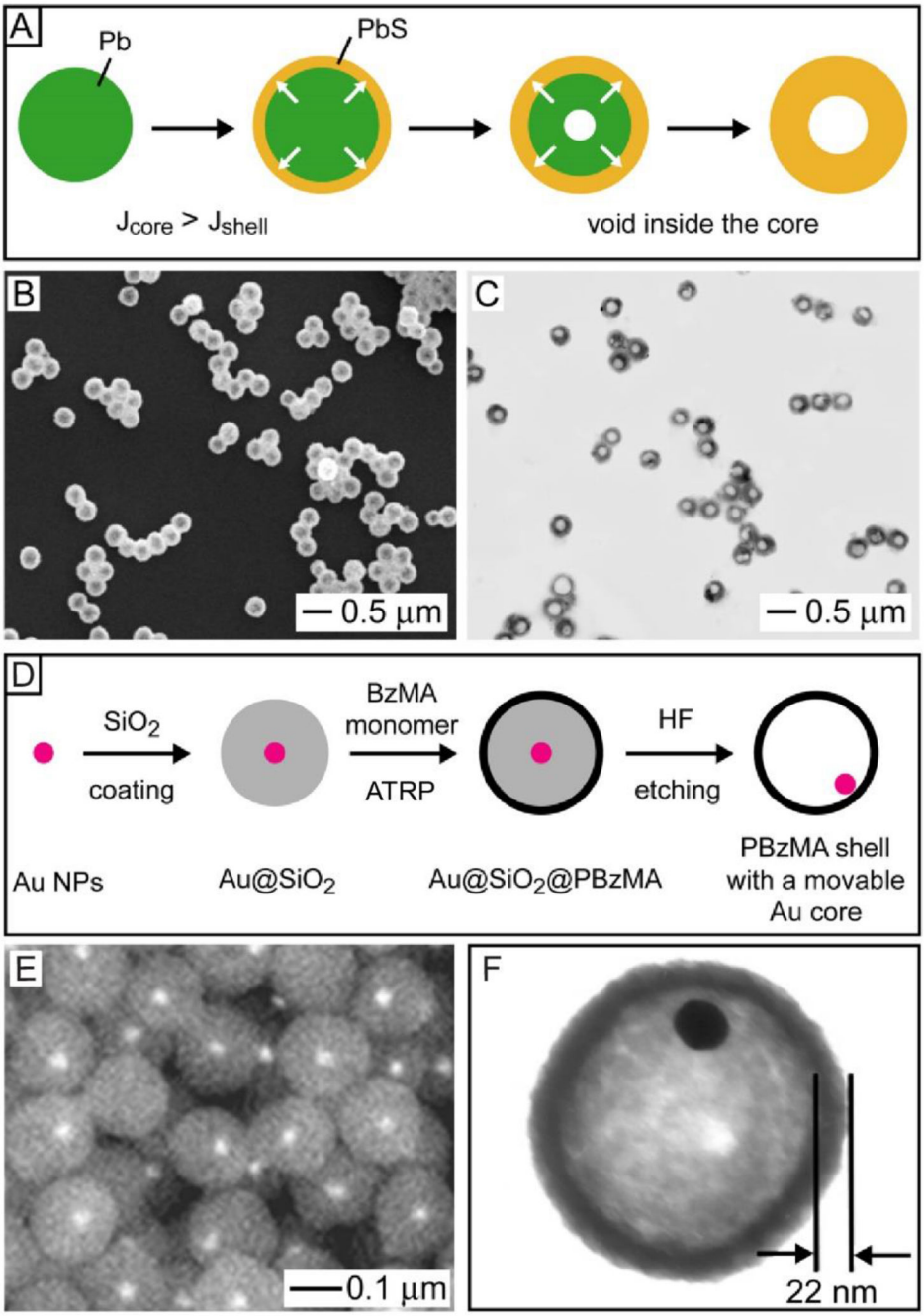


**Figure 3.**

(A) Schematic showing the synthesis of a PbS hollow sphere from a Pb sphere through the Kirkendall effect. $J_{core}$ and $J_{shell}$ refer to the material flow flux from the core to the shell and from the shell to the core, respectively. (B) SEM and (C) TEM images of the PbS hollow spheres prepared by reacting Pb spheres with sulfur under the protection of Ar. (D) Schematic showing the formation of a PBzMA hollow sphere containing a movable Au nanoparticle in the interior. (E) Backscattering SEM and (F) TEM images of the as-obtained

PBzMA hollow spheres. Reproduced with permission from (A-C) ref 18 and (D-F) ref 20. Copyright 2005 Wiley-VCH and 2003 American Chemical Society, respectively.

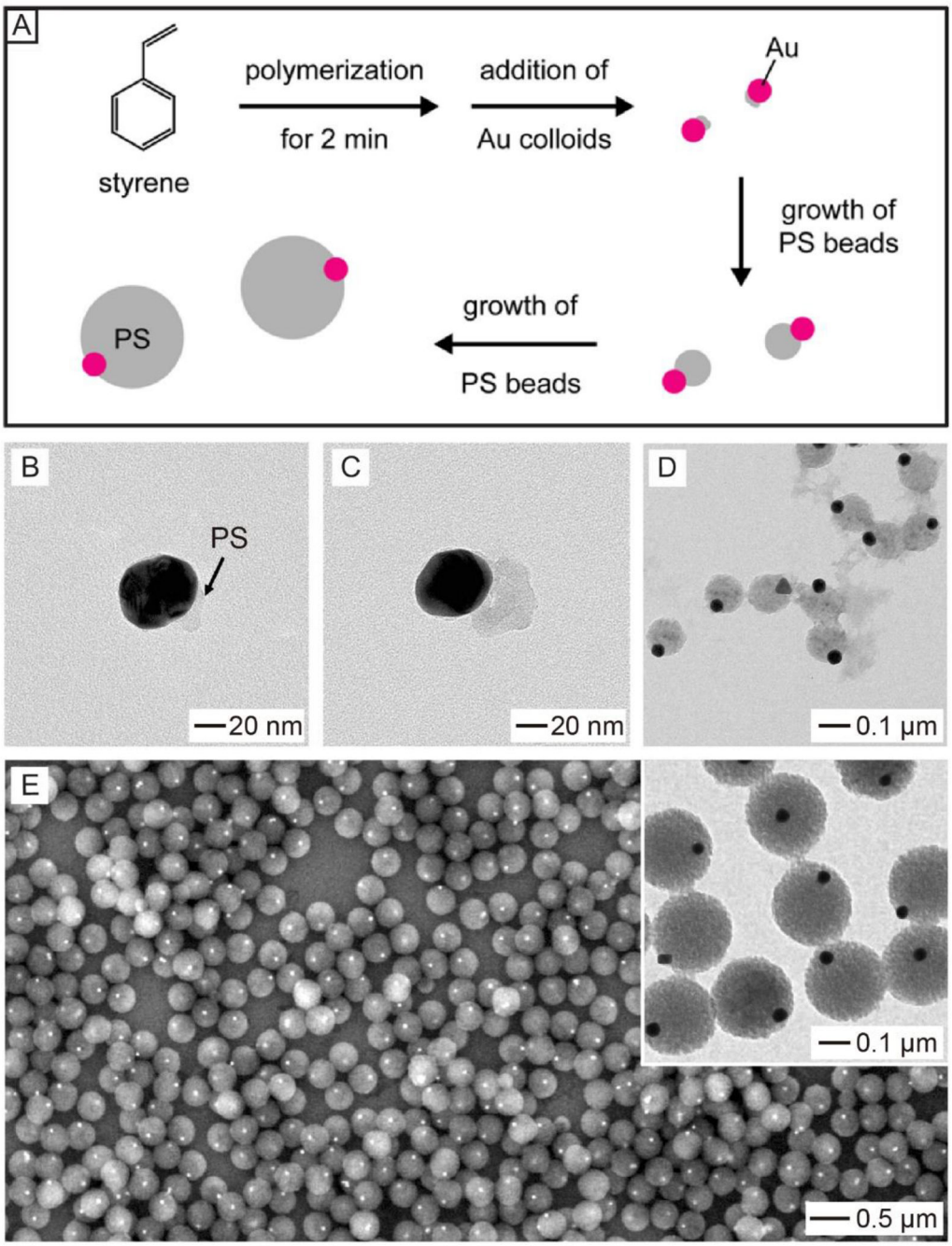


**Figure 4.**

(A) Schematic showing the synthesis of Au-PS colloidal spheres with a Janus structure through the precipitation polymerization of styrene in the presence of Au nanoparticles as seeds. (B-D) TEM images of the intermediate products after the reaction had proceeded for (B) 5, (C) 10, and (D) 30 min, confirming that PS only grew from one side of the Au nanoparticle. (E) SEM and TEM images (inset) of the final Au-PS Janus particles. Reproduced with permission from ref 25. Copyright 2009 American Chemical Society.

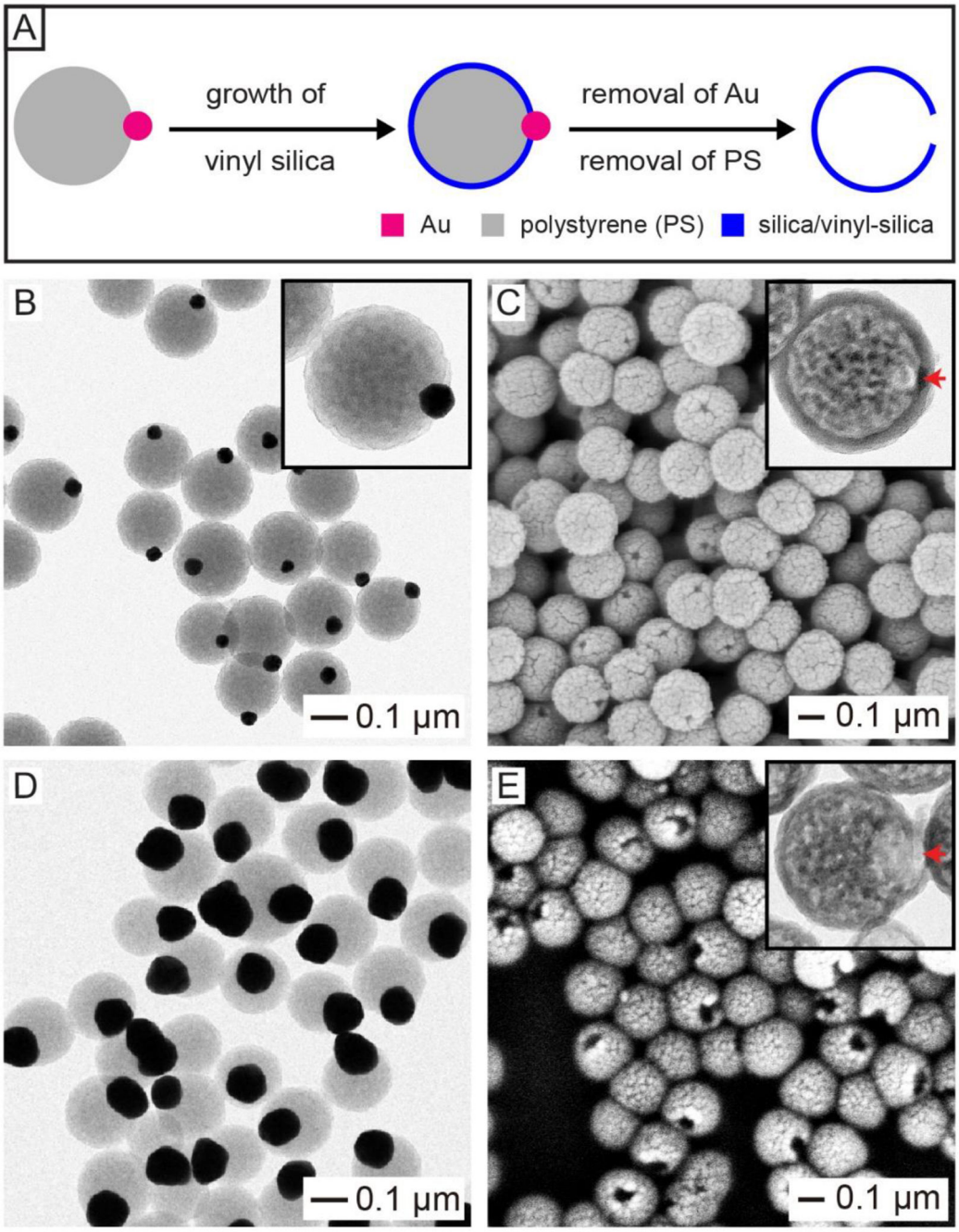


**Figure 5.**

(A) Schematic showing the synthesis of a hollow silica/vinyl-silica sphere with a hole in the wall through site-selected deposition by templating with the Au-PS Janus particle. (B, D) TEM images of Au-PS particles containing (B) 50- and (D) 100-nm Au nanoparticles. (C, E) SEM images of the as-obtained hollow silica spheres by templating with Au-PS Janus particles in (B, D), respectively. The insets show TEM images of the corresponding samples. Reproduced with permission from ref 27. Copyright 2019 Wiley-VCH.

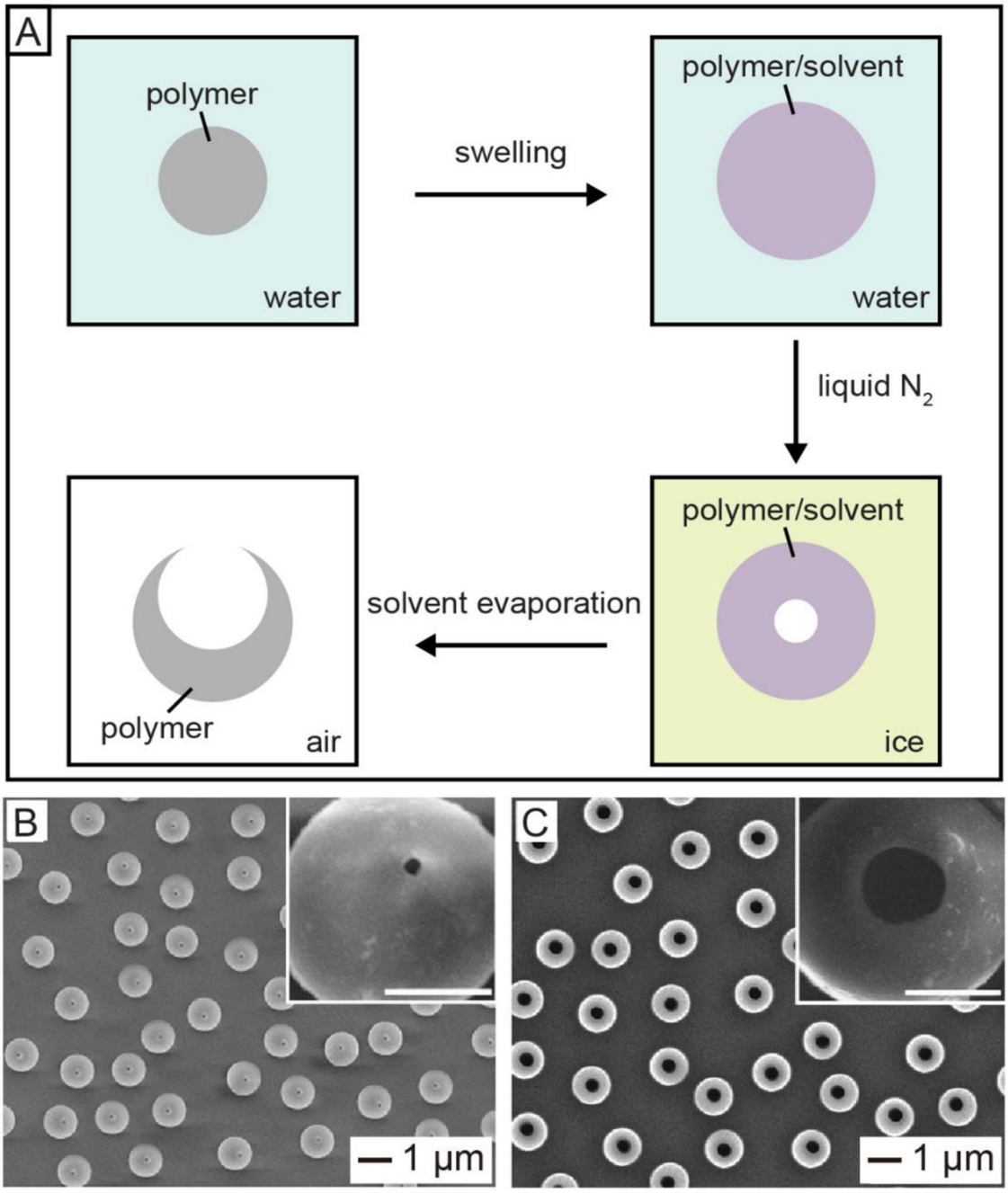


**Figure 6.**

(A) Schematic illustration showing the transformation of a solid polymer bead into a hollow sphere with a hole on the surface. (B, C) SEM images of the hollow PS spheres with openings of (B) 50 and (C) 350 nm in diameter by swelling commercial PS beads with different concentrations of styrene, followed by freeze-drying. Reproduced with permission from (A) ref 30 and (B, C) ref 31. Copyright 2005 Springer Nature and 2013 Wiley-VCH, respectively.

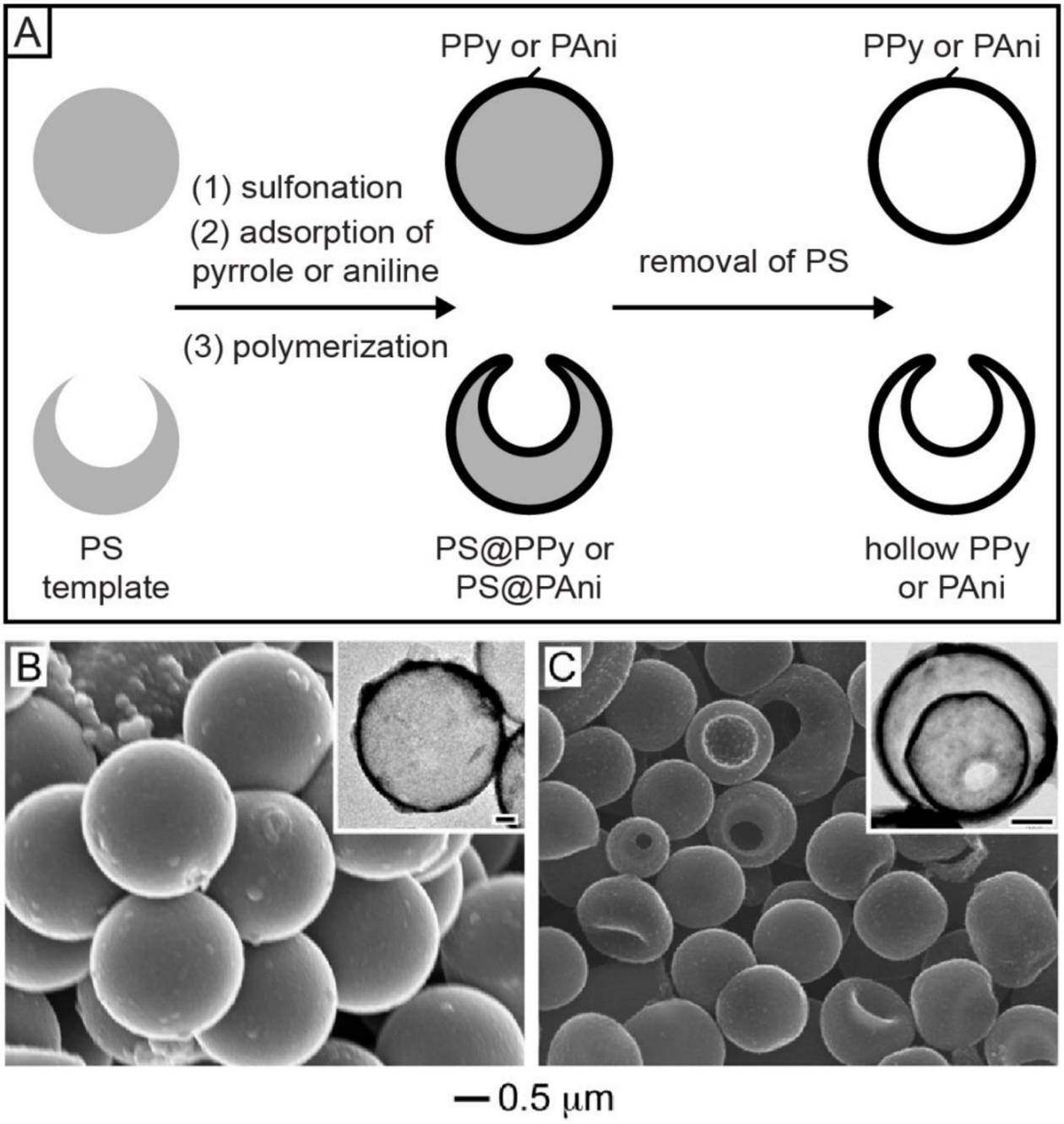


**Figure 7.**

(A) Schematic showing the preparation of single-, double-, and triple-walled hollow spheres made of conducting polymers (PPy or PAni) by templating with PS beads and PS hollow spheres with a hole on the surface, respectively. (B) SEM image of PS@PPy core-shell spheres. The inset shows the TEM image of a PPy hollow sphere obtained after removing the PS. (C) SEM image of triple-walled PPy hollow spheres. The inset shows the TEM image of a double-walled PPy hollow sphere obtained after the removal of PS. The scale

bars in the insets correspond to 0.3 μm. Adapted with permission from (B) ref 34 and (C) ref 35. Copyright 2009 and 2010 Wiley-VCH, respectively.

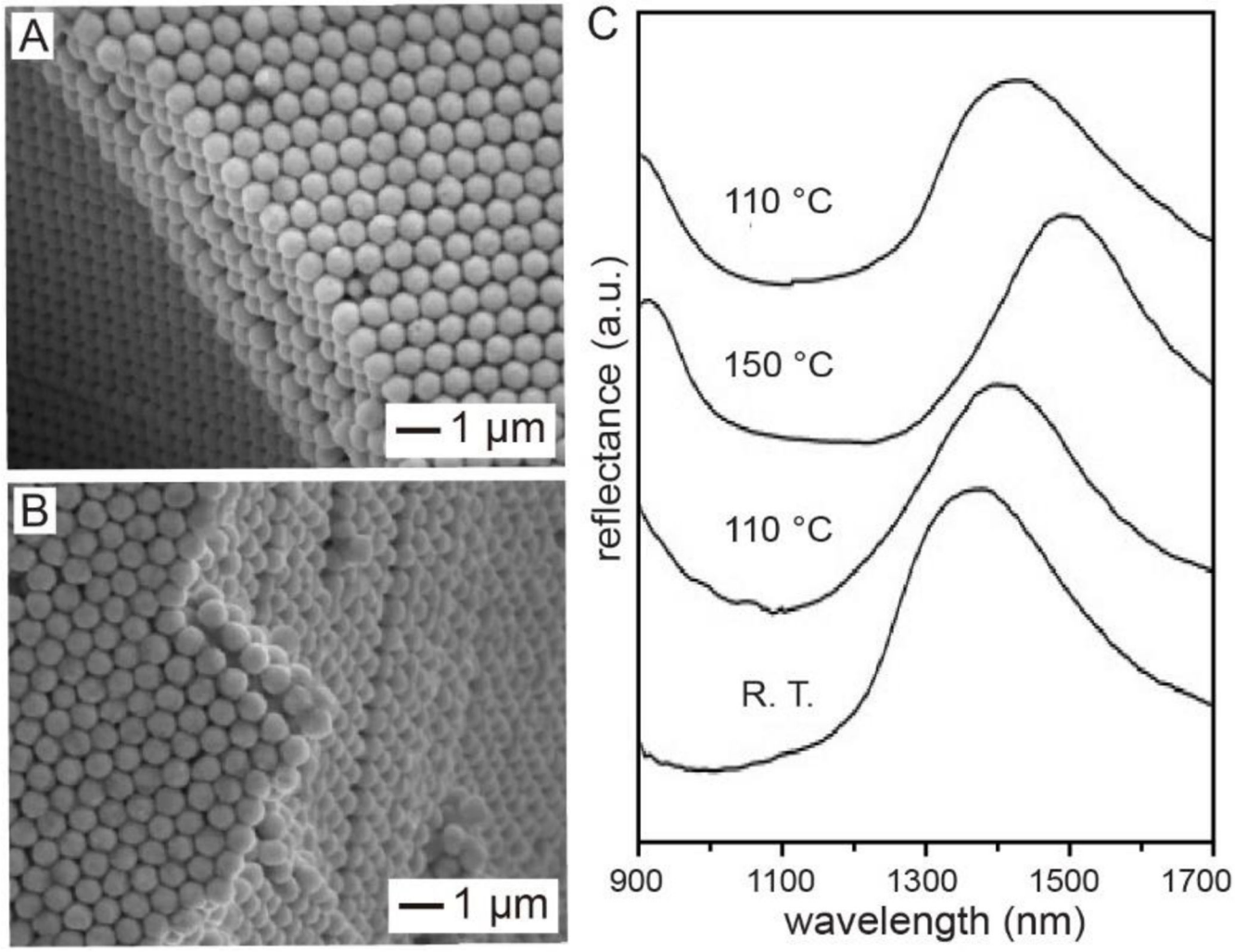


**Figure 8.**

(A) SEM images of a crystalline lattice assembled from *a*-Se@$Ag_2Se$ core-shell colloidal spheres. (B) SEM image of the same crystal after it had been annealed at 150 °C for 10 min. (C) Reflectance spectra recorded from an *a*-Se@$Ag_2Se$ crystal. The temperature was increased from room temperature (R.T.) to 110 and 150 °C, respectively, and then reduced to 110 °C. Reproduced with permission from ref 15. Copyright 2005 Wiley-VCH.

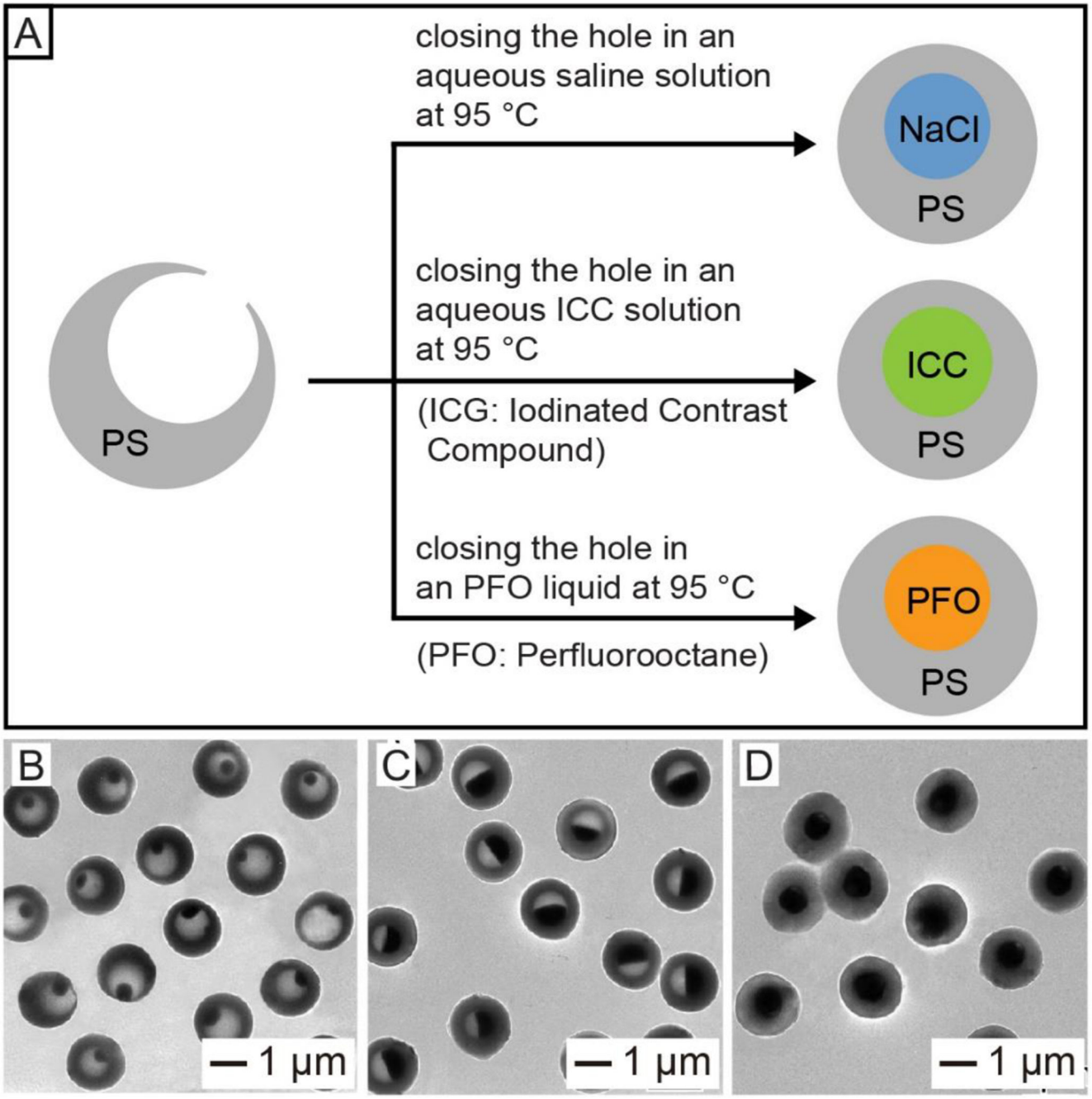


**Figure 9.**

(A) Schematic showing the encapsulation of imaging contrast agents in PS hollow spheres by thermally closing the hole in the surface. (B–D) TEM images of PS hollow spheres after encapsulation of aqueous ioversol solutions at different concentrations of (A) 25%, (B) 51%, and (C) 74%. The holes were closed by heating the PS hollow spheres at 95 °C for 45 min in an aqueous solution. Reproduced with permission from ref 41. Copyright 2012 Wiley-VCH.

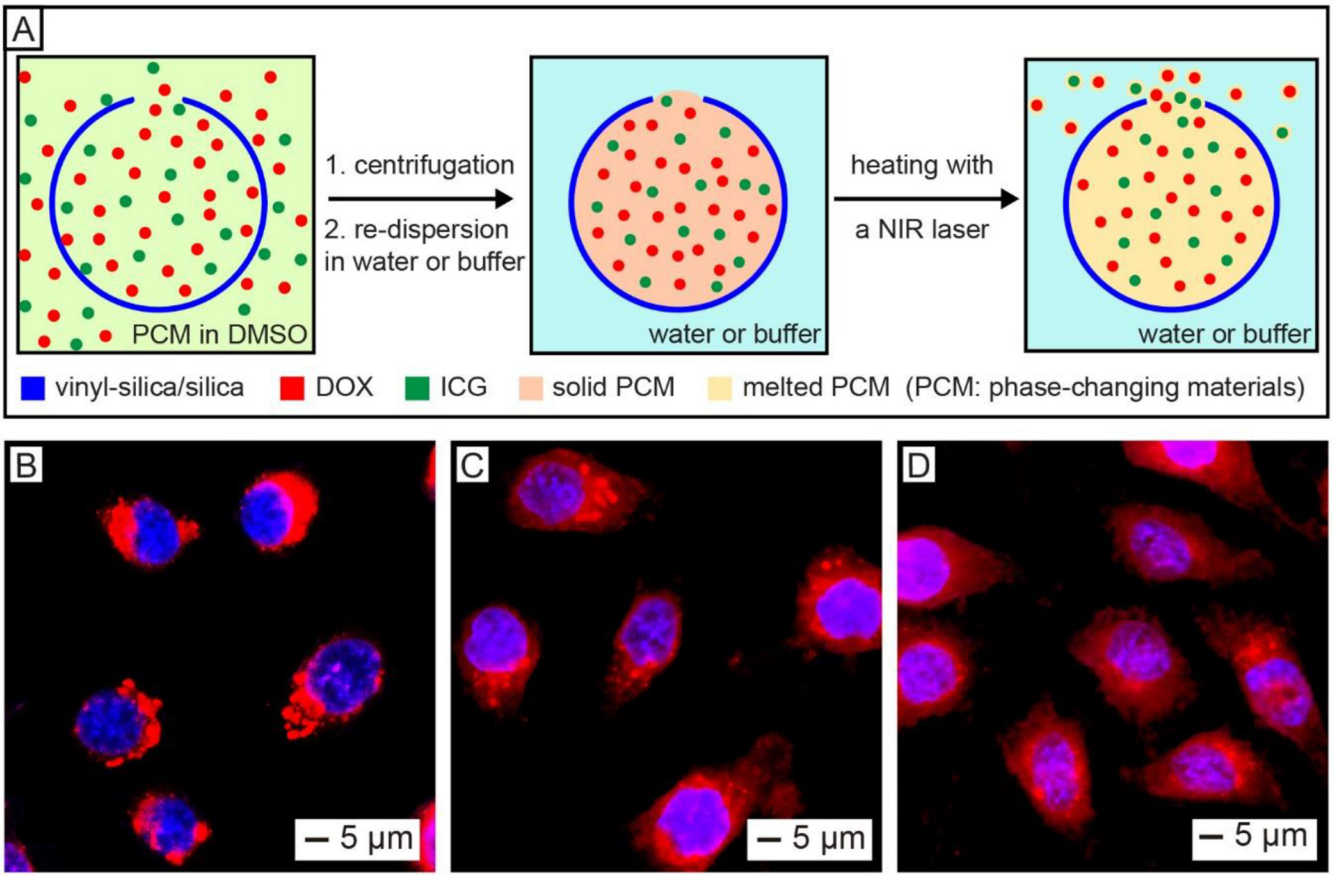


**Figure 10.**

(A) Schematic showing the co-loading of drug (DOX), NIR dye (ICG), and PCM into a hollow silica sphere with a hole in the wall for NIR-controlled release. (B–D) Fluorescence images of HeLa cells after incubation with the hollow spheres loaded with DOX, ICG, and PCM: (B) without laser irradiation, (C) after laser irradiation for 8 min, and (D) after three rounds of 8-min laser irradiation. The appearance of red fluorescence in nuclei upon laser irradiation indicates the release of the loaded drug. The laser had an output peaked at 808 nm, together with an irradiance of 0.4 W $cm^{-2}$. Reproduced with permission from ref 27. Copyright 2019 Wiley-VCH.